Original Article

Neoadjuvant programmed death-1 blockade plus chemotherapy in locally advanced esophageal squamous cell carcinoma

Guozhen Yang[1,2,3#], Xiaodong Su[1,2,3#], Hong Yang[1,2,3#], Guangyu Luo[1,4], Chan Gao[5], Yating Zheng[5], Wenzhuan Xie[5], Mengli Huang[5], Ting Bei[5]^, Yuezong Bai[5], Zhiqiang Wang[1,6], Peiqiang Cai[1,7], Haoqiang He[1,7], Jin Xiang[1,8], Muyan Cai[1,8], Yijun Zhang[1,8], Chunhua Qu[1,8], Jianhua Fu[1,2,3], Qianwen Liu[1,2,3], Yi Hu[1,2,3], Jiudi Zhong[1,2,3], Yuanheng Huang[1,2,3], Qiyu Guo[1,2,3], Xu Zhang[1,2,3]

[1]State Key Laboratory of Oncology in South China, Collaborative Innovation Center of Cancer Medicine, Guangzhou, China; [2]Guangdong Esophageal Cancer Institute, Guangzhou, China; [3]Department of Thoracic Oncology, Sun Yat-sen University Cancer Center, Guangzhou, China; [4]Department of Endoscopy, Sun Yat-sen University Cancer Center, Guangzhou, China; [5]Medical Affairs, 3D Medicines, Inc., Shanghai, China; [6]Department of Medical Oncology, Sun Yat-sen University Cancer Center, Guangzhou, China; [7]Department of Medical Imaging and Interventional Radiology, Sun Yat-sen University Cancer Center, Guangzhou, China; [8]Department of Pathology, Sun Yat-sen University Cancer Center, Guangzhou, China

Contributions: (I) Conception and design: X Zhang, G Yang; (II) Administrative support: X Zhang, G Yang; (III) Provision of study materials or patients: All authors; (IV) Collection and assembly of data: All authors; (V) Data analysis and interpretation: All authors; (VI) Manuscript writing: All authors; (VII) Final approval of manuscript: All authors.

[#]These authors contributed equally to this work.

Correspondence to: Xu Zhang, MD, PhD, Department of Thoracic Oncology, State Key Laboratory of Oncology in South China, Collaborative Innovation Center of Cancer Medicine, Guangdong Esophageal Cancer Institute, Sun Yat-sen University Cancer Center, 651 Dong Feng Road East, Guangzhou 510060, China. Email: zhangxu@sysucc.org.cn.

Background: Immunotherapy is effective in treating unresectable esophageal squamous cell carcinoma (ESCC), but little is known about its role in the preoperative setting. The aim of this study was to evaluate the safety, feasibility and efficacy of neoadjuvant treatment with camrelizumab plus chemotherapy in locally advanced ESCC.

Methods: Patients diagnosed with locally advanced ESCC were retrospectively included if they had received neoadjuvant camrelizumab plus nab-paclitaxel and S1 capsule followed by radical esophagectomy between November, 2019 and June, 2020 at Sun Yat-sen University Cancer Center. Primary endpoints were safety and feasibility. In addition, pathological response and the relationship between tumor immune microenvironment (TIME)/tumor mutational burden (TMB) and treatment response were also investigated.

Results: Twelve patients were included and they all received three courses of preoperative treatment with camrelizumab plus nab-paclitaxel/S1. No grade 3 or higher toxicities occurred. No surgical delay or perioperative death was reported. Nine patients (75%) responded to the treatment, four with a complete pathological response (pCR) and five with a major pathological response (MPR). Neither programmed death-ligand 1 (PD-L1) expression nor TMB was correlated with treatment response. TIME analysis revealed that a higher abundance of CD56dim natural killer cells was associated with better pathological response in the primary tumor, while lower density of M2-tumor-associated macrophages was associated with better pathological response in the lymph nodes (LNs).

Conclusions: Neoadjuvant camrelizumab plus nab-paclitaxel and S1 is safe, feasible and effective in locally advanced ESCC and is worth further investigation.

Keywords: Anti-programmed death-1 (PD-1); esophageal squamous cell carcinoma (ESCC); neoadjuvant therapy; tumor immune microenvironment (TIME); tumor mutational burden (TMB)

^ ORCID: 0000-0001-7481-2202.

Submitted Jun 11, 2021. Accepted for publication Aug 05, 2021.
doi: 10.21037/atm-21-3352
View this article at: https://dx.doi.org/10.21037/atm-21-3352

Introduction

With over 500,000 new cases diagnosed annually, esophageal carcinoma ranks as the seventh most common cancer worldwide and the sixth leading cause of cancer deaths in 2018 (1). Approximately 90% of all esophageal cancers are esophageal squamous cell carcinomas (ESCCs) (2). For patients diagnosed with locally advanced ESCC, preoperative chemoradiation followed by surgery is available as the standard-of-care treatment, but recurrence still occurs in 31–39% of patients within 3–5 years after surgery (3,4). Moreover, the increased risk of perioperative toxicities, complications and mortality associated with chemoradiation makes it less appealing to a vast number of patients (5,6).

In recent years, anti-programmed death-1 (PD-1)/anti-programmed death-ligand 1 (PD-L1) has demonstrated great promise in unresectable ESCC patients, and thus has been approved by the Food and Drug Administration as second-line treatment in this population (7,8). In addition, neoadjuvant administration of anti-PD-1 in other malignancies such as lung cancer, melanoma and colorectal cancer has also produced durable responses with favorable tolerability (9-11). Multiple trials are therefore currently underway to exploit preoperative use of anti-PD-1/PD-L1 in locally advanced ESCC, most of which combined anti-PD-1/PD-L1 with chemotherapy or chemoradiation. However, according to the preliminary data presented by Lee *et al.* at ESMO Congress 2019, upon preoperative administration of pembrolizumab plus platinum-based chemoradiotherapy, eight deaths (out of 28 patients) occurred, two due to pre-surgical hematemesis, two resulting from acute lung injury, and four due to disease progression (12). Despite a 46.1% complete pathological response (pCR) rate among the patients having undergone surgery, anti-PD-1 combined with chemoradiation raised considerable safety concerns. Therefore, a less toxic regimen is needed in this scenario.

This retrospective analysis investigates the safety and feasibility of neoadjuvant treatment with camrelizumab plus nab-paclitaxel and S1 in a small cohort of patients with locally advanced ESCC. Treatment responses assessed by radiography were also evaluated in comparison with surgical pathology. Since predictive biomarkers predicting treatment response are urgently needed to be identified, the correlation between tumor immune microenvironment (TIME)/tumor mutational burden (TMB) and treatment response was also explored. We present the following article in accordance with the STROBE reporting checklist (available at https://dx.doi.org/10.21037/atm-21-3352).

Methods

Patients and study design

ESCC patients who received camrelizumab plus nab-paclitaxel and S1 before standard radical esophagectomy between November, 2019 and June, 2020 at Sun Yat-sen University Cancer Center were retrospectively screened. They were included if they had: (I) a diagnosis of stage T2–3, N0–3 locally advanced ESCC confirmed with contrast-enhanced computerized tomography (CT), EUS, and cervical lymph node (LN) ultrasonography; (II) no cervical LN metastasis or distant organ metastasis; and (III) no secondary primary tumors. All patients were subjected to post-treatment evaluation using contrast-enhanced CT and cervical LN ultrasonography within seven days before surgery. Patients' de-identified data were extracted from their electronic medical records.

The primary endpoints of the study were safety and feasibility. The secondary end points were radiographic and pathological responses. An exploratory objective of this study was to identify genomic and immunologic features that may predict benefit from neoadjuvant immunochemotherapy in locally advanced ESCC. This study was approved by the institutional review boards at Sun Yat-sen University Cancer Center (B2020-292-01) and all patients provided written informed consents. All procedures performed in this study involving human participants were in accordance with the Declaration of Helsinki (as revised in 2013).

Assessment

Treatment-related adverse events (TRAEs) were reported according to the National Cancer Institute Common

Terminology Criteria for Adverse Events, version 5.0 (13). Feasibility was defined as no surgical delay due to immune-related TRAEs and no severe perioperative complications. Radiographic responses of primary tumors were evaluated using CT scan images acquired before and after neoadjuvant treatment per Response Evaluation Criteria in Solid Tumors version (RECIST) 1.1 (14). Pathological regression was assessed using hematoxylin and eosin (H&E) stained slides of surgical specimens. Tumors with ≤10% residual viable tumor cells were considered as having achieved a major pathological response (MPR) while those showing no residual tumor were defined as having a pCR. Patients with ≥50% remaining viable tumor were classified as non-responders. All imaging data and pathological data were reviewed by two independent radiologists or pathologists.

TIME

Investigation of the TIME was performed by 3D Medicines, Inc, a College of American Pathologists (CAP)-accredited and Clinical Laboratory Improvement Amendments (CLIA)-certified laboratory. PD-L1 expression was assessed using the PD-L1 IHC 22C3 pharmDx assay (Agilent Technologies, CA, USA) and was expressed as combined positive score (CPS) by dividing the number of PD-L1-stained tumor and immune cells with the total number of viable tumor cells and multiplying by 100. Multiplex immunofluorescence (mIF) staining was conducted using the PANO 7-plex IHC kit following manufacturer's instructions (Panovue, Beijing, China). Multiplex stained slides were scanned using a Mantra system (PerkinElmer, MA, USA) configured to capture fluorescent spectra at 20 nm wavelength intervals from 420 nm to 720 nm with a fixed exposure time and an absolute magnification of ×200 and ×100. All scans for each slide were then superimposed to obtain a single image. Images of unstained and monoplex stained slides were used to extract tissue autofluorescence and the spectrum of each fluorophore, respectively. They were also used to create a spectral library required for multispectral unmixing using the inForm Image Analysis software v.2.4 (PerkinElmer, MA, USA). Slide images were reconstructed without autofluorescence using this spectral library. The quantity of CD8+ T cells, macrophages and natural killer cells were expressed as the number of stained cells per square millimeter.

Next generation sequencing (NGS) and TMB determination

NGS was performed on pretreatment tissues as described previously using the GPS panel targeting the exons of 733 selected cancer-related genes (3D Medicines Inc., Shanghai, China) (see Table S1 for a full list of the 733 genes included in the panel) (15). Briefly, genomic DNA (gDNA) was isolated from formalin-fixed paraffin-embedded (FFPE) tissue sections with a ≥20% tumor content using the ReliaPrep FFPE gDNA Miniprep System (Promega). DNA extracts (30–200 ng) were sheared to 250 bp fragments using a S220 focused-ultrasonicator (Covaris, Inc., MA, USA). Libraries were prepared using the KAPA Hyper Prep Kit (KAPA Biosystems, Cape Town, South Africa) following the manufacturer's protocol, followed by probe-based hybridization with a customized NGS panel targeting exons of 733 cancer-related genes. The captured libraries were loaded onto a NovaSeq 6000 platform (Illumina, CA, USA) for 100 bp paired-end sequencing with a mean sequencing depth of 1,000×. Somatic single nucleotide variants (SNVs) were detected using MuTect (v1.1.7) (https://github.com/broadinstitute/mutect) and somatic insertions and deletions (indels) using Pindel (v0.2.5a8) (http://gmt.genome.wustl.edu/packages/pindel) with default parameters. Copy number variations (CNVs) were called by an in-house developed script with a cut-off of 6 copies. The TMB was defined as the number of somatic single nucleotide variations (SNVs) and insertions/deletions (indels) per megabase of coding genome sequenced. SNVs referred to synonymous & non-synonymous mutations, stop gain/loss, and splicing variants. Indels included both frameshift and non-frameshift insertions and deletions. Non-coding alterations were excluded from TMB calculation.

Statistical analyses

Continuous variables were compared using Mann-Whitney U test and categorical variables were compared using Chi-square or Fisher exact test. All reported P values were two-tailed. A P value of <0.05 is considered statistically significant. All analyses and graph generation were

Table 1 Baseline characteristic of the patients

Characteristics	No. (%)
Age at diagnosis, years	
Mean ± S[a]	57±5.5
Median [range]	56 [50–65]
Gender	
Male	7 (58.3)
Female	5 (41.7)
History of smoking	
Former or current	7 (58.3)
Never	5 (41.7)
Site of primary tumor	
Upper thoracic	1 (8.3)
Middle thoracic	6 (50.0)
Lower thoracic	5 (41.7)
Histologic grade	
Well differentiated	1 (8.3)
Moderately differentiated	3 (25.0)
Poorly differentiated	8 (66.7)
Tumor stage[b]	
II	2 (16.7)
III	8 (66.6)
IVA	2 (16.7)
PD-L1 CPS	
<10	9 (75.0)
≥10	2 (16.7)
Unevaluable	1 (8.3)

[a], standard deviation; [b], tumor stage was evaluated following the American Joint Committee on Cancer's (AJCC) Staging Manual, 7th edition. PD-L1, programmed death-ligand 1; CPS, combined positive score.

performed using R 3.6.0.

Results

Baseline characteristics

A total of 12 ESCC patients who agreed to receive preoperative anti-PD-1 plus nab-paclitaxel and S1 before radical esophagectomy between November, 2019 and June, 2020 were included in the study (*Table 1*). In all, seven were males and five were females. The median age of the cohort was 56 years (range, 50–65 years). Two patients had stage II, eight had stage III and two had stage IVA ESCC. Two-thirds of the patients had poorly differentiated tumors (see Table S2 for baseline clinicophysiological characteristics of the patients). All patients completed three courses of preoperative treatment which comprised a flat dose of camrelizumab (200 mg, IVGTT) plus a single dose of nab-paclitaxel (260 mg/m^2, IVGTT) on day 1 and S1 administered twice daily [40 mg for body surface area (BSA) <1.25 m^2, 50 mg for BSA ≥1.25 to <1.50 m^2, or 60 mg for BSA ≥1.50 m^2] on days 1 to 14. The cycle was repeated every three weeks for three cycles.

Safety and feasibility

Neoadjuvant use of camrelizumab in combination with nab-paclitaxel and S1 did not cause any previously unreported toxicities (*Table 2*). All patients experienced at least one TRAE, but no grade 3 or higher events occurred. Overall, the most common grade 1–2 events included reactive capillary hemangioma of the skin (91.7%), muscle soreness (50.0%), limb numbness (41.7%), and anemia (16.7%), among which reactive capillary hemangioma was immune-related. Toxicities such as pneumonia, myocarditis, hepatitis, nephritis, thyroiditis and hypophysitis that are usually associated with immunotherapy were not observed. All TRAEs resolved without intervention.

All patients underwent thoracoscopic esophagectomy with cervical esophagogastric anastomosis and modern two-field LN dissection as planned. The median interval between the last dose of neoadjuvant therapy and surgery was 1.2 weeks (range, 0.4–2.9 weeks) and all patients underwent standard R0 resection, which took 253.0±28.4 minutes on average. Intraoperative bleeding volume was 50–200 mL. No perioperative mortality was reported. Anastomotic leakage occurred in two patients 10 and 11 days after surgery, respectively, and both were healed after one week of conservative treatment. None of the patients experienced any postoperative immune-related adverse events or other complications.

Clinical and pathological responses

According to RECIST v1.1, seven (58.3%) patients had partial response (PR) and five (41.7%) had stable disease (SD) (*Figure 1A*). Surgical pathology showed a median

Table 2 Summary of treatment related adverse events

All events	No. of patients (%)	
	Grade 1–2	Grade 3–4
Gastrointestinal		
Nausea	1 (8.3)	0 (0)
Vomiting	1 (8.3)	0 (0)
Diarrhea	1 (8.3)	0 (0)
Constipation	1 (8.3)	0 (0)
ALT/AST increase	0 (0)	0 (0)
Hematopoietic		
Anemia	2 (16.7)	0 (0)
Leukopenia	0 (0)	0 (0)
Thrombocytopenia	0 (0)	0 (0)
Respiratory system		
Cough	0 (0)	0 (0)
Pneumonia	0 (0)	0 (0)
Peripheral nerve		
Limb numbness	5 (41.7)	0 (0)
Muscle soreness	6 (50.0)	0 (0)
Cardiac troponin	0 (0)	0 (0)
Immune-related adverse events		
Reactive capillary hemangioma	11 (91.7)	0 (0)
Myocarditis	0 (0)	0 (0)
Hepatitis	0 (0)	0 (0)
Nephritis	0 (0)	0 (0)
Pneumonia	0 (0)	0 (0)
Hyperthyroidism	0 (0)	0 (0)
Hypophysitis	0 (0)	0 (0)

All adverse events were reported according to the National Cancer Institute Common Terminology Criteria for Adverse Events, version 5.0.

tumor regression of 97% (range, 4–100%). Four patients achieved a pCR and five cases had an MPR in the primary tumor, which were collectively defined as responders (75%) (*Figure 1B*). The other three patients only displayed a regression of 30, 4% and 4%, respectively, and were therefore regarded as non-responders. Ten patients had down-staging in the primary tumors and nine of the 11 patients with potential LN involvement according to baseline CT showed LN down-staging (see Table S2, which summarizes potential baseline LN involvement by CT). None of the pCR patients had LN metastasis following treatment.

Five patients exhibited discordant radiographic and pathological responses. Two had SD according to presurgical CT but were found to have an MPR and a pCR, respectively. Three of the PR patients turned out to have a pCR in resected tissue. This was consistent with previous observation that evaluation per RECIST criteria may not truly reflect actual benefit from immunotherapy (9). Of note, the surgical resections of the responders showed an inflamed phenotype with a massive influx of multinucleated giant cells and lymphocytes compared to baseline biopsy samples, a phenomenon typically associated with response to immune checkpoint blockade, which may help explain the minimal tumor shrinkage or even tumor enlargement seen in the CT scans of some responders (*Figure 1C*). Tertiary lymphoid structures (TLSs), which predicted favorable prognosis and improved response to immunotherapy in several solid tumors, were also observed in the resected tumor of responders, corroborating the favorable responses in these patients (16-18).

Tumor regression pattern induced by anti-PD-1-based neoadjuvant therapy

Tumor regression as revealed by surgical pathology seemed to follow a sequential pattern. Non-responders still showed invasion through the mucosa into the muscularis propria or adventitia (*Figure 2A* Right, *Table 3*). Among the five MPR patients, those without invasion in the muscularis were also free of tumor in the adventitia (patients 5 and 7) while those without invasion in the submucosa were also free of tumor in the muscularis and adventitia (patients 6 and 8), suggesting that regression induced by anti-PD-1-based neoadjuvant therapy may start from the outermost layer and extend towards the innermost layer of the esophageal wall (*Figure 2B*).

Immunologic and genomic correlates of response to anti-PD-1-based neoadjuvant therapy

In KEYNOTE-180, a CPS PD-L1 of ≥10 was associated with a slight improvement of objective response rate in advanced esophageal cancer, therefore we also examined PD-L1 expression in our cohort (8). Among the

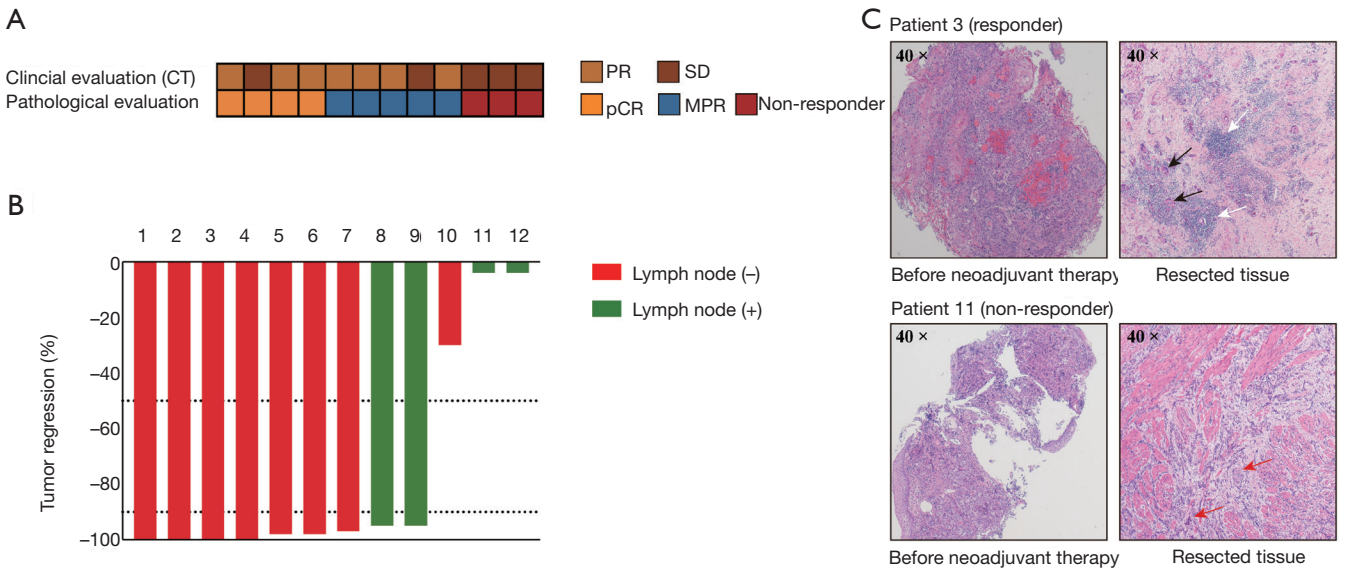

Figure 1 Clinical and pathological responses to neoadjuvant treatment. (A) Response assessment with CT and surgical pathology. (B) Pathological tumor regression in the resected primary tumor. Green and red denote the presence and absence of lymph node metastases, respectively. The upper and lower dashed lines indicate 50 and 90 regression, respectively. (C) Representative hematoxylin and eosin-stained sections of tumor tissue obtained before neoadjuvant therapy and after surgery (resected tissue) from a patient with pCR (patient 3) and a non-responder (patient 11). Black arrows indicate multinucleated giant cells; white arrows indicate tertiary lymphoid structures; red arrows indicate neoplastic cells. Patient 3 and patient 11 were representative of pCR patients and non-responders, respectively. CT, computerized tomography; pCR, complete pathological response. Images are shown at 40× magnification.

11 tumors evaluable for PD-L1 expression, only two had a CPS of ≥10, one MPR and one non-responder, while all pCR patients had a CPS of <10 (*Figure 3A*). TMB was also analyzed given its increasing importance for guiding immunotherapy in solid tumors. However, no statistically significant difference in TMB was detected between responders and non-responders. Moreover, the 11 tumors were subjected to mIF to get a glimpse of their TIME. The densities of CD8+ T cells, TAMs (M1 and M2), and NK cells ($CD56^{bright}$ and $CD56^{dim}$) were quantified. $CD56^{dim}$ NK cells were significantly more abundant in the responders than in the non-responders (221.12±76.83 *vs.* 52.33±11.05, P=0.02) (*Figure 3B,3C*). Among patients demonstrating LN down-staging, those who also achieved pCR in the LNs (LN pCR) had significantly more M2-TAMs in the primary tumors than those without LN pCR (LN non-PCR) (85.29±21.56 *vs.* 437.67±113.28, P=0.02) (*Figure 3D,3E*). No differences were observed in the densities of CD8+ T cells, M1-TAMs, and $CD56^{bright}$ NK cells between responders and non-responders or between LN pCR and LN non-pCR patients (data not shown).

Discussion

Our study showed that neoadjuvant treatment of locally advanced ESCC patients with camrelizumab plus nab-paclitaxel and S-1 was well tolerated without causing any grade 3 or higher TRAEs, any surgical delay or any severe perioperative complications. Four patients achieved a pCR and five had a MPR. Radiographic and pathological responses were discrepant for 5/12 cases. Neither PD-L1 expression nor TMB was correlated with treatment response and analysis of TIME showed association between the abundance of $CD56^{dim}$ NK cells and M2-TAMs with pathological response in the primary tumors and in the LNs, respectively.

In the preoperative setting, platinum-based chemotherapy plus radiotherapy represents the current standard of care and has been adopted as the combination partner of immunotherapy by a number of ongoing trials (19,20). However, the safety concerns associated with radiotherapy prompted us to seek a less toxic regimen (12,21,22). In lung squamous cell carcinoma, preoperative

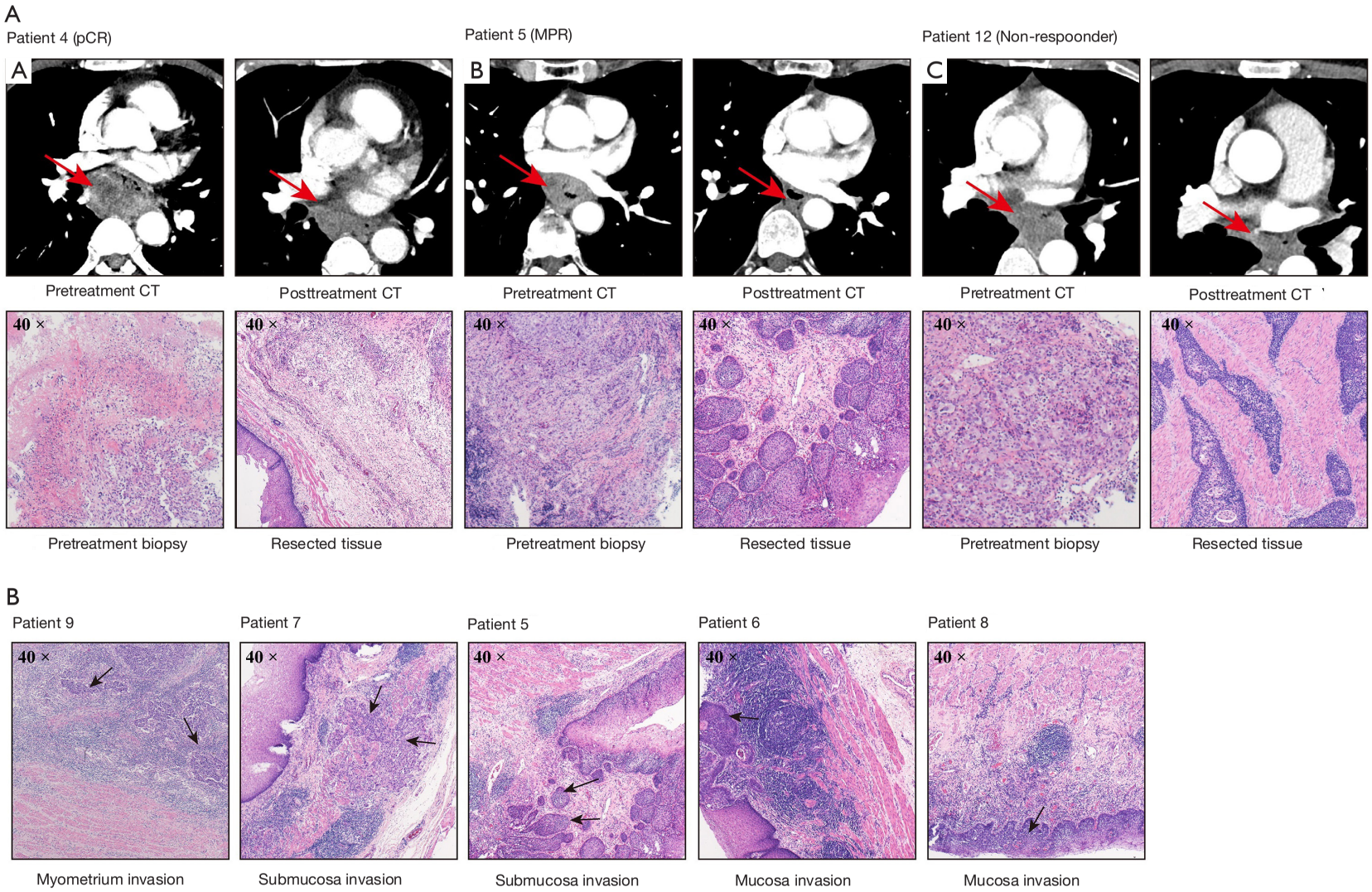

Figure 2 Patterns of tumor regression in radiography and pathology following neoadjuvant therapy. (A) CT scans (top), EUS images (middle), and hematoxylin and eosin-stained sections of surgical tissue (bottom) of patient 4 who had a pCR (left), patient 5 who had a MPR (middle), and patient 12 who was a non-responder (right). Red arrows indicate tumor lesions. (B) Representative surgical hematoxylin and eosin-stained sections of the MPR patients showing residual tumor in the muscularis propria (patient 9), submucosa (patients 7 and 5), and mucosa (patients 6 and 8). Black arrows indicate viable tumor cells. CT, computerized tomography; pCR, complete pathological response; MPR, major pathological response.

Table 3 Tumor regression evaluated by radiography, endoscopic ultrasonography, and surgical pathology

Patient	Radiographic evaluation	Pathological evaluation
#1	PR	pCR
#2	SD	pCR
#3	PR	pCR
#4	PR	pCR
#5	PR	MPR, residual tumor in submucosa and mucosa
#6	PR	MPR, residual tumor in mucosa
#7	PR	MPR, residual tumor in submucosa and mucosa
#8	SD	MPR, residual tumor in mucosa
#9	PR	MPR, residual tumor in inner muscularis, submucosa and mucosa
#10	SD	Non-responder, residual tumor in muscularis, submucosa, and mucosa
#11	SD	Non-responder, residual tumor in adventitia, muscularis, submucosa, and mucosa
#12	SD	Non-responder, residual tumor in adventitia, muscularis, submucosa, and mucosa

PR, partial response; SD, stable disease; pCR, complete pathological response; MPR, major pathological response.

atezolizumab combined with nab-paclitaxel and carboplatin was able to induce a 50% pCR with manageable toxicities (23). Therefore, we were interested to see how ESCC would respond to immunotherapy plus chemotherapy. Indeed, in our study, neoadjuvant administration of nab-paclitaxel plus S1 in conjunction with camrelizumab, a PD-1 inhibitor approved for second-line treatment of unresectable ESCC in China, demonstrated an excellent safety profile and induced at least 90% tumor regression in 75% of the patients. Another study recently presented at ESMO congress 2020 employed a similar regimen comprising nab-paclitaxel/S1 plus toripalimab for preoperative treatment of a similar population, but their pCR rate (16.67%) was much lower than ours, which could possibly be explained by the fact that their cohort received only two courses of treatment before surgery while our entire cohort was subjected to 3 cycles of treatment (24).

In another study conducted by Shen *et al.*, the pCR elicited by neoadjuvant PD-1 plus chemotherapy was 33%, which was exactly the same as ours (25). Actually, our study does differ from theirs. A rather homogenous PD-1 inhibitor regimen, camrelizumab was employed in our study. In contrast, in Shen *et al.*'s study, patients received PD-1 inhibitors such as nivolumab, pembrolizumab, or camrelizumab, which may have elicited different effects. Secondly, the number of cycles of neoadjuvant treatment in our study was three, which was one more than the two in their research. Several phase 3 trials investigating lung cancer in the neoadjuvant setting have extended the treatment cycle to 3–4 cycles (ClinicalTrials.gov No. NCT03425643, NCT03456063, and NCT03800134). Our results suggest that three cycles of treatment did not increase toxicities of the combinatorial neoadjuvant immune-chemotherapy in locally advanced ESCC.

LN metastasis is closely associated with poor prognosis in ESCC, but a substantial fraction of patients remains ypN-positive after neoadjuvant treatment, which may later drive postsurgical relapse (26). In our cohort, LN down-staging co-occurred with primary tumor down-staging in nine patients, of which the three pCR patients who had potential baseline LN involvement also achieved pCR in the LNs, indicating that for these patients, incorporation of anti-PD-1 may not only induce anti-tumor immune response in the primary tumor, but also enhance systemic priming of the immune system to eradicate micrometastases in other tissues such as LNs. This notion is also supported by previous evidence in non-small cell lung cancer that some T-cell clones infiltrating pretreatment tumors were also found in the peripheral blood and resected LNs following PD-1 blockade (9).

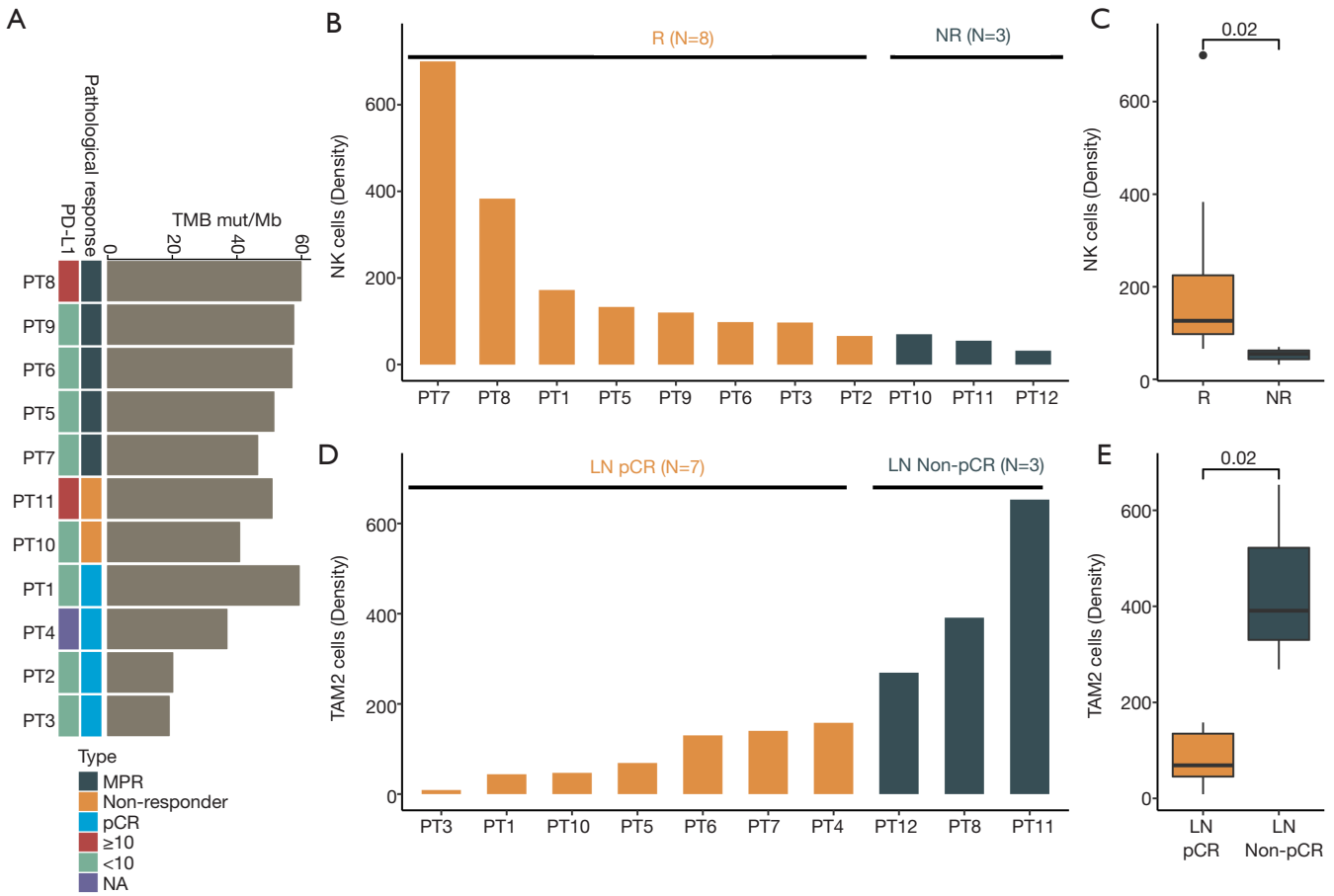

Figure 3 Correlation between TIME and pathological response. (A) Tumor mutational burden and PD-L1 expression among the responders and non-responders as assessed by next generation sequencing with a 733-gene panel and by PD-L1 IHC 22C3 pharmDx assay. (B,C) Density of natural killer cells in the responders (R) (221.12±76.83) *vs.* the NR (52.33±11.05) (P=0.02 by exact Wilcoxon test). (D,E) Density of M2-like tumor-associated macrophages in the patients with complete pathological response in the LNs (pCR) (437.67±113.28) *vs.* patients without complete pathological response in the lymph nodes (85.29±21.56) (P=0.02 by exact Wilcoxon test). Density was defined as the number of stained cells per square millimeter. TIME, tumor immune microenvironment; PD-L1, programmed death-ligand 1; NR, non-responders; LN, lymph node; pCR, complete pathological response.

Despite the approval of pembrolizumab in advanced esophageal cancer with a CPS PD-L1 of ≥10 and in advanced solid tumors with a TMB of ≥10 mutations/megabase, the roles of PD-L1 and TMB as predictors of immune checkpoint blockade remained to be clarified (20). Indeed, our observations showed poor correlation of PD-L1 expression or TMB with pathological response to neoadjuvant immunochemotherapy. It is therefore important to explore other biomarkers to guide patient selection. Consistent with previous literature showing positive correlation between NK cell abundance and clinical response to nivolumab in advanced melanoma, NK cells were found at a higher density in the responders in our cohort (27). Moreover, these NK cells belonged to the $CD56^{dim}$ subset, the mature form of NK cells with more potent antitumor effects, which may help explain the favorable response in the responders (28). In addition, M2-TAMs were more abundant in patients who remained LN-positive after neoadjuvant treatment. This is supported by the fact that M2-TAMs may subvert immune surveillance by producing immune-suppressing cytokines, rendering the patients resistant to immunotherapy (29).

Our study was limited by its retrospective design and a small sample size. However, we included a rather

homogenous population where treatment regimen and schedule were both consistent across the entire cohort, which to some extent ensured data quality. Secondly, the follow-up time was too short for us to fully assess the impact of favorable pathological responses on recurrence-free and overall survivals. A larger phase II study with long-term follow-up is currently underway to confirm our findings in a prospective manner (ChiCTR2000029807). Taken together, neoadjuvant administration of PD-1 blockade in combination with chemotherapy was tolerable, feasible, and efficacious in locally advanced ESCC.

Acknowledgments

The authors would like to acknowledge all patients participating in the study.
Funding: This study was supported by the Science and Technology Planning Project of Guangdong Province of China (2017A020215179) and the Science and Technology Planning Project of Guangzhou of China (202103000064).

Footnote

Reporting Checklist: The authors have completed the STROBE reporting checklist. Available at https://dx.doi.org/10.21037/atm-21-3352

Data Sharing Statement: Available at https://dx.doi.org/10.21037/atm-21-3352

Conflicts of Interest: All authors have completed the ICMJE uniform disclosure form (available at https://dx.doi.org/10.21037/atm-21-3352). Dr. CG, YZ, WX, MH, TB, and YB are employees of 3D Medicines Inc. The other authors have no other conflicts of interest to declare.

Ethical Statement: The authors are accountable for all aspects of the work in ensuring that questions related to the accuracy or integrity of any part of the work are appropriately investigated and resolved. This study was approved by the institutional review boards at Sun Yat-sen University Cancer Center (B2020-292-01) and all patients provided written informed consents. All procedures performed in this study involving human participants were in accordance with the Declaration of Helsinki (as revised in 2013).

References

1. Bray F, Ferlay J, Soerjomataram I, et al. Global cancer statistics 2018: GLOBOCAN estimates of incidence and mortality worldwide for 36 cancers in 185 countries. CA Cancer J Clin 2018;68:394-424.
2. Abnet CC, Arnold M, Wei WQ. Epidemiology of Esophageal Squamous Cell Carcinoma. Gastroenterology 2018;154:360-73.
3. Kong M, Shen J, Zhou C, et al. Prognostic factors for survival in esophageal squamous cell carcinoma (ESCC) patients with a complete regression of the primary tumor (ypT0) after neoadjuvant chemoradiotherapy (NCRT) followed by surgery. Ann Transl Med 2020;8:1129.
4. Xi M, Yang Y, Zhang L, et al. Multi-institutional Analysis of Recurrence and Survival After Neoadjuvant Chemoradiotherapy of Esophageal Cancer: Impact of Histology on Recurrence Patterns and Outcomes. Ann Surg 2019;269:663-70.
5. Deng J, Xia Y, Chen Y, et al. Long term results of different radiotherapy techniques and fractions for esophageal squamous cell carcinoma. Transl Cancer Res 2020;9:2287-94.
6. Liedman B, Johnsson E, Merke C, et al. Preoperative adjuvant radiochemotherapy may increase the risk in patients undergoing thoracoabdominal esophageal resections. Dig Surg 2001;18:169-75.
7. Kato K, Cho BC, Takahashi M, et al. Nivolumab versus chemotherapy in patients with advanced oesophageal squamous cell carcinoma refractory or intolerant to previous chemotherapy (ATTRACTION-3): a multicentre, randomised, open-label, phase 3 trial. Lancet Oncol 2019;20:1506-17.
8. Shah MA, Adenis A, Enzinger PC, et al. Pembrolizumab versus chemotherapy as second-line therapy for advanced esophageal cancer: Phase 3 KEYNOTE-181 study. J Clin Oncol 2019;37:abstr 4010.
9. Liang W, Cai K, Chen C, et al. Expert consensus on neoadjuvant immunotherapy for non-small cell lung

cancer. Transl Lung Cancer Res 2020;9:2696-715.
10. Chalabi M, Fanchi LF, Dijkstra KK, et al. Neoadjuvant immunotherapy leads to pathological responses in MMR-proficient and MMR-deficient early-stage colon cancers. Nat Med 2020;26:566-76.
11. Amaria RN, Reddy SM, Tawbi HA, et al. Neoadjuvant immune checkpoint blockade in high-risk resectable melanoma. Nat Med 2018;24:1649-54.
12. Lee S, Ahn BC, Park SY, et al. A phase II trial of preoperative chemoradiotherapy and pembrolizumab for locally advanced esophageal squamous cell carcinoma (ESCC). J Clin Oncol 2019;37:abstr 4027.
13. National Cancer Institute Common Terminology Criteria for Adverse Events (CTCAE), version 5.0 for adverse event reporting 2019.
14. Eisenhauer EA, Therasse P, Bogaerts J, et al. New response evaluation criteria in solid tumours: revised RECIST guideline (version 1.1). Eur J Cancer 2009;45:228-47.
15. Su D, Zhang D, Chen K, et al. High performance of targeted next generation sequencing on variance detection in clinical tumor specimens in comparison with current conventional methods. J Exp Clin Cancer Res 2017;36:121.
16. Cabrita R, Lauss M, Sanna A, et al. Tertiary lymphoid structures improve immunotherapy and survival in melanoma. Nature 2020;577:561-5.
17. Helmink BA, Reddy SM, Gao J, et al. B cells and tertiary lymphoid structures promote immunotherapy response. Nature 2020;577:549-55.
18. Gao J, Navai N, Alhalabi O, et al. Neoadjuvant PD-L1 plus CTLA-4 blockade in patients with cisplatin-ineligible operable high-risk urothelial carcinoma. Nat Med 2020;26:1845-51.
19. Ajani JA, D'Amico TA, Bentrem DJ, et al. Esophageal and Esophagogastric Junction Cancers, Version 2.2019, NCCN Clinical Practice Guidelines in Oncology. J Natl Compr Canc Netw 2019;17:855-83.
20. Vivaldi C, Catanese S, Massa V, et al. Immune Checkpoint Inhibitors in Esophageal Cancers: are we Finally Finding the Right Path in the Mist? Int J Mol Sci 2020;21:1658.
21. Hartmann JT, Lipp HP. Toxicity of platinum compounds. Expert Opin Pharmacother 2003;4:889-901.
22. Giuranno L, Ient J, De Ruysscher D, et al. Radiation-Induced Lung Injury (RILI). Front Oncol 2019;9:877.
23. Shu CA, Gainor JF, Awad MM, et al. Neoadjuvant atezolizumab and chemotherapy in patients with resectable non-small-cell lung cancer: an open-label, multicentre, single-arm, phase 2 trial. Lancet Oncol 2020;21:786-95.
24. Zhang G, Hu Y, Yang B, et al. A single-centre, prospective, open-label, single-arm trial of toripalimab with nab-paclitaxel and S-1 as a neoadjuvant therapy for esophageal squamous cell carcinoma (ESCC). Ann Oncol 2020;31:S645-71.
25. Shen D, Chen Q, Wu J, et al. The safety and efficacy of neoadjuvant PD-1 inhibitor with chemotherapy for locally advanced esophageal squamous cell carcinoma. J Gastrointest Oncol 2021;12:1-10.
26. Leng X, He W, Yang H, et al. Prognostic Impact of Postoperative Lymph Node Metastases After Neoadjuvant Chemoradiotherapy for Locally Advanced Squamous Cell Carcinoma of Esophagus: From the Results of NEOCRTEC5010, a Randomized Multicenter Study. Ann Surg 2019. [Epub ahead of print]. doi: 10.1097/SLA.0000000000003727.
27. Riaz N, Havel JJ, Makarov V, et al. Tumor and Microenvironment Evolution during Immunotherapy with Nivolumab. Cell 2017;171:934-949.e16.
28. Wagner JA, Rosario M, Romee R, et al. CD56bright NK cells exhibit potent antitumor responses following IL-15 priming. J Clin Invest 2017;127:4042-58.
29. Li X, Liu R, Su X, et al. Harnessing tumor-associated macrophages as aids for cancer immunotherapy. Mol Cancer 2019;18:177.

(English Language Editor: G. Stone)

Cite this article as: Yang G, Su X, Yang H, Luo G, Gao C, Zheng Y, Xie W, Huang M, Bei T, Bai Y, Wang Z, Cai P, He H, Xiang J, Cai M, Zhang Y, Qu C, Fu J, Liu Q, Hu Y, Zhong J, Huang Y, Guo Q, Zhang X. Neoadjuvant programmed death-1 blockade plus chemotherapy in locally advanced esophageal squamous cell carcinoma. Ann Transl Med 2021;9(15):1254. doi: 10.21037/atm-21-3352

Table S1 List of genes of the 733-gene panel

ABL1	CDX2	FGFR4	MLH1	PTEN	VEGFA	JMJD1C	TRIM37	BCL11A	EZR	TBL1XR1	PLXNB1	LIG1	RNF168	POLD3
ACVR2A	CHD2	FH	MLLT3	PTK6	VHL	LMO1	TSHR	BCL11B	FAT4	TCF7L2	SPRED1	LIG3	RNF4	POLD4
AFF3	CHEK1	FHIT	MPL	PTPRD	NSD3	LZTR1	UROD	BCORL1	FUBP1	TCL1A	ERF	LIG4	RNF8	POLE2
AKT1	CHEK2	FLCN	MRE11A	RAC1	ZNF479	MAX	WAS	BIRC3	FUS	TET1	RPS6KA3	MAD2L2	RPA1	POLE4
AKT2	CHIC2	FLT1	MSH2	RAD50	ZNRF3	MEN1	WRN	BRD4	GAS7	TFE3	GSK3B	MBD4	RPA2	PPP4R1
AKT3	CIC	FLT3	MSH3	RAD51	ABCB11	MTAP	WT1	CACNA1D	H3F3A	TNFAIP3	NOTCH3	MDC1	RPA3	PPP4R3A
ALK	CIITA	FLT4	MSH6	RAD51C	APOBEC3B	MUTYH	XPA	CALR	HIF1A	USP8	NOTCH4	MGMT	RPA4	PPP4R3B
ANK1	CRBN	FOXA1	MTOR	RAF1	AXIN2	NBN	XPC	CAMTA1	HIP1	WIF1	ALKBH2	MLH3	RRM2B	PPP4R4
APC	CRLF2	FRS2	MYC	RARA	BARD1	NHP2	XRCC2	CANT1	HNRNPA2B1	XPO1	ALKBH3	MMS19	SETMAR	RAD9B
AR	CRNKL1	G6PD	MYCN	RB1	BMPR1A	NME1	HOXB13	CARD11	HOXA11	ZFHX3	APEX1	MNAT1	SEM1	RBX1
ARAF	CRTC3	GATA3	MYD88	RET	BUB1B	NOP10	BCL2L1	KNL1	IL6ST	ACVR1B	APEX2	MPG	SHPRH	RFC1
AREG	CSF1R	GLI2	NF1	RGS7	CDC73	NTHL1	BCL6	CASP8	KDM6A	ARID1B	CENPS	MSH4	SMUG1	RFC2
ARHGAP5	CSF3R	GNA11	NF2	RICTOR	CDKN1C	PHOX2B	CDK8	CBFA2T3	KEAP1	DNMT1	APLF	MUS81	SPO11	RFC3
ARID1A	CTNNB1	GNAQ	NFE2L2	RNF43	CEBPA	PMS1	FOXP1	CBFB	KLF4	FOXL2	APTX	NEIL1	TDG	RFC4
ARNT	CTNND2	GNAS	NFIB	ROS1	COL7A1	POLH	GRIN2A	CBLB	LCK	GATA1	ATRIP	NEIL2	TDP1	TELO2
ASXL1	CUL3	HDAC2	NKX2-1	RPTOR	CTR9	POLQ	IKBKE	CCDC6	LEF1	HIST1H3B	FAAP100	NEIL3	TDP2	TIMELESS
ATM	CYSLTR2	HEY1	NOTCH1	RUNX1	CXCR4	POT1	MEF2B	CCNB1IP1	LIFR	KDM5C	FAAP24	NHEJ1	TOP3A	TMEM189
ATR	DDR2	HGF	NOTCH2	SDC4	CYLD	PRDM9	NFKBIA	CD79A	MAPK1	MAP3K1	FAAP20	NUDT1	TOP3B	WDR48
AURKA	DICER1	HOOK3	NPM1	SDHC	DDB2	PRF1	PIK3CD	CD79B	MED12	KMT2C	MPLKIP	NABP2	TOPBP1	GFI1
AXL	DNMT3A	HRAS	NRAS	SERPINB3	DIS3L2	PRKAR1A	SRC	CDH11	NAB2	NCOR1	CCNH	OGG1	TP53BP1	CYP17A1
B2M	DPYD	IDH1	NRG1	SETD2	DKC1	PRSS1	BTG1	CHD4	NCOR2	PHF6	CDK7	PARP1	TREX1	ELF3
BAP1	EGFR	IDH2	NTRK1	SF3B1	DOCK8	PTPN11	DIS3	CLIP1	NDRG1	PPP2R1A	CETN2	PARP2	TREX2	SGK1
BAZ1A	EPHA2	IGF1R	NTRK2	SH2B3	DROSHA	PTPN13	EED	CLTCL1	NONO	PRDM1	CHAF1A	PARP3	UBE2A	GSTT1
BCL2	EPHA3	IGF2	NTRK3	SLC29A1	ELANE	RAD51B	GNA13	CNBP	PAX3	SOCS1	CLK2	PCNA	UBE2B	AEN
BCOR	ERBB2	IL7R	PAK1	SMAD4	EPCAM	RAD51D	NT5C2	CNOT3	PAX7	SOX9	DCLRE1A	PNKP	UBE2N	CCNO
BLM	ERBB3	INPP4B	PALB2	SMARCA1	ERCC3	RECQL	PPP2R2A	CREB3L1	PAX8	TRAF7	DCLRE1B	POLB	UBE2T	CENPX
BMP5	ERBB4	ITGAV	PAX5	SMARCA4	ERCC5	RECQL4	NSD2	CREB3L2	PER1	IKZF1	DCLRE1C	POLI	UBE2V2	CUL4A
BRAF	ERCC1	JAK1	PBRM1	SMARCB1	ETV6	RFWD3	EPHA7	CREBBP	PICALM	MYCL	DDB1	POLK	UNG	CUL5
BRCA1	ERCC2	JAK2	PDCD1LG2	SMO	EXT1	RHBDF2	GLI1	CRTC1	PIM1	NCOA3	DMC1	POLL	USP1	DNTT
BRCA2	ERCC4	JAK3	PDGFB	SRGAP3	EXT2	SBDS	MYB	CTCF	POU2AF1	CDK2	DUT	POLM	XAB2	ELOA
BRIP1	ERCC6	JUN	PDGFRA	SRSF2	FAH	SDHA	NRG3	CUX1	POU5F1	LATS1	EME1	POLN	XRCC1	HUS1B
BTK	EREG	KCNJ5	PDGFRB	STAG2	FANCD2	SDHAF2	NUP93	DAXX	PPP6C	LATS2	EME2	PRKDC	XRCC3	PER2
CARS	ESR1	KDR	PDPK1	STK11	FANCE	SDHB	PTK2	DDIT3	PRDM16	YAP1	ENDOV	PRPF19	XRCC4	PER3
CBL	EWSR1	KIT	PIK3CA	SUZ12	FANCF	SDHD	RXRA	DDX10	PREX2	TEAD2	ERCC8	RAD1	XRCC5	MSH5
CCND1	EZH2	KMT2A	PIK3CB	SYK	FANCI	SERPINA1	SMARCA2	DDX3X	PRKACA	MGA	EXO1	RAD18	XRCC6	PARP4
CCND2	FAM135B	KMT2D	PIK3R1	TBX3	FANCL	SETBP1	TYK2	DDX5	PTPRT	HES1	FAN1	RAD23A	ABRAXAS1	POLE3
CCND3	FAM47C	KRAS	PIK3R2	TCF3	FANCM	SH2D1A	ZNF750	DDX6	QKI	KDM5A	FANCB	RAD23B	FRK	PPP4R2
CCNE1	FANCA	LASP1	PLCG2	TERT	FAS	SHOC2	ABI1	DNM2	RAD21	SPEN	GEN1	RAD52	BIRC5	SLX1A
CD274	FANCC	LMNA	PML	TET2	FEN1	SLC25A13	ACKR3	EBF1	RANBP2	THBS2	GTF2H1	RAD54B	EMSY	RAD54L2
CDH1	FANCG	LRP1B	PMS2	TMEM127	GALNT12	SLX4	ACSL3	EIF3E	RAP1GDS1	CUL1	GTF2H3	RAD54L	CRKL	RFC5
CDH10	FAT1	MAP2K1	POLD1	TMPRSS2	GATA2	SOS1	ACVR1	EIF4A2	RBM10	HDAC1	GTF2H4	RAD9A	EPHB1	HMGA2
CDK12	FBXW7	MAP2K2	POLE	TOP2A	GBA	SPOP	AFF4	ELF4	RHOA	MLST8	GTF2H5	RBBP8	GLI3	TSPAN31
CDK4	FES	MAP2K4	POLG	TP53	GJB2	SPRTN	AMER1	ELK4	RHOH	PIK3R3	H2AFX	RDM1	IRS2	MYOD1
CDK6	FGF19	MCL1	PPARG	TPMT	GPC3	SRY	ARID2	ELL	RNF213	RHEB	HELQ	RECQL5	RUNX1T1	CHD1
CDKN1A	FGF3	MDM2	PPM1D	TSC1	GREM1	STAT3	ATP1A1	EP300	SFPQ	RPS6KB1	HFM1	REV1	SLIT2	ZBTB16
CDKN1B	FGF4	MDM4	PRCC	TSC2	HFE	SUFU	ATP2B3	EPAS1	SLC34A2	GRB2	HLTF	REV3L	SOX2	PCDH9
CDKN2A	FGFR1	MECOM	PRKCH	U2AF1	HMBS	TGFBR1	ATRX	EPS15	SLC45A3	RIT1	HMGB1	RIF1	SPTA1	PLXNA1
CDKN2B	FGFR2	MET	PSIP1	UGT1A1	HNF1A	TGFBR2	AXIN1	ERC1	SMAD2	RASA1	HUS1	RMI1	ZNF217	
CDKN2C	FGFR3	MITF	PTCH1	USP6	ITK	TP63	BCL10	ETNK1	SMAD3	ERRFI1	UVSSA	RMI2	ZNF703	

Table S2 Clinicophysiological characteristics of the patients

No.	Gender	Age	Smoking[a]	Drinking[a]	Site of primary tumor	Differentiation	cTNM[e]	Clinical response[c]	pTNM[e]	Pathological response[f]	T downstage	N downstage	No. of LND[b]	No. of LNM[d]
1	Male	56	Y	Y	Middle	Well	cT2N2M0 III	PR	pT0N0M0	pCR	Y	Y	34	0
2	Female	60	N	N	Middle	Moderately	cT3N0M0 II	SD	pT0N0M0	pCR	Y	-	26	0
3	Female	65	N	N	Middle	Poorly	cT3N1M0 III	PR	pT0N0M0	pCR	Y	Y	34	0
4	Male	56	N	N	Lower	Poorly	cT3N1M0 III	PR	pT0N0M0	pCR	Y	Y	24	0
5	Male	51	Y	Y	Lower	Poorly	cT3N1M0 III	PR	pT1bN0M0	MPR	Y	Y	30	0
6	Male	51	Y	Y	Upper	Moderately	cT2N2M0 III	PR	pTisN0M0	MPR	Y	Y	28	0
7	Male	63	Y	Y	Lower	Poorly	cT2N1M0 II	PR	pT1bN0M0	MPR	Y	Y	63	0
8	Male	50	Y	Y	Middle	Moderately	cT3N3M0 IVA	SD	pTisN1M0	MPR	Y	Y	50	1
9	Male	56	Y	Y	Lower	Poorly	cT3N3M0 IVA	PR	pT2N2M0	MPR	Y	Y	54	3
10	Female	62	Y	Y	Lower	Poorly	cT3N2M0 III	SD	pT2N0M0	Non-responder	Y	Y	35	0
11	Female	63	N	N	Middle	Poorly	cT3N1M0 III	SD	pT3N1M0	Non-responder	N	N	27	1
12	Female	51	N	N	Middle	Poorly	cT3N2M0 III	SD	pT3N2M0	Non-responder	N	N	61	4

[a], Y: yes. N: no; [b], LND: lymph node dissected; [c], clinical response was evaluated according to the Response evaluation Criteria in solid tumors (RECIST) v1.1; [d], LNM: lymph node metastasis; [e], clinical stage and pathological stage were evaluated according to the criteria of the American Joint Committee on Cancer, seventh edition; [f], pCR is defined as no residual viable tumor cells remaining, MPR is defined as ≤10% viable tumor cells remaining, non-responder is defined as ≥50% residual viable tumor cells.